

Full-length article

Enzymatic activity characterization of SARS coronavirus 3C-like protease by fluorescence resonance energy transfer technique¹

Shuai CHEN², Li-li CHEN², Hai-bin LUO, Tao SUN, Jing CHEN, Fei YE, Jian-hua CAI, Jing-kang SHEN, Xu SHEN³, Hua-liang JIANG³

Drug Discovery and Design Center, State Key Laboratory of Drug Research, Shanghai Institute of Materia Medica, Shanghai Institutes for Biological Sciences, Chinese Academy of Sciences, Graduate School of the Chinese Academy of Sciences, Shanghai 201203, China

Key words

severe acute respiratory coronavirus; 3C-like protease; fluorescence resonance energy transfer; fluorogenic substrate; enzyme activity; site-directed mutagenesis

¹ Project supported by the State Key Program of Basic Research of China (grants 2003-CB514125, 2003CB514124, 2002CB512807, 2002CB512802, 2002AA233011), Sino-European Project on SARS Diagnostics and Antivirals (Proposal/Contract No 003831), and the special programs of oppugning SARS from the Ministry of Science and Technology, Chinese Academy of Sciences, National Natural Science Foundation of China and Shanghai Science and Technology Commission.

² Authors contributed equally to this work.

³ Correspondence to Prof. Xu SHEN, Prof Hua-liang JIANG.
Phn 86-21-5080-6600. Fax 86-21-5080-7088.
E-mail xshen@mail.shnc.ac.cn, hljiang@mail.shnc.ac.cn

Received 2004-05-31

Accepted 2004-09-01

doi: 10.1111/j.1745-7254.2005.00010.x

Introduction

Between the end of 2002 and June 2003, a severe epidemic disease called severe acute respiratory syndrome (SARS) broke out in China and quickly spread to more than 30 other countries. A novel coronavirus, SARS-CoV, was identified as the etiological agent of SARS infection by using biophysical and biochemical techniques^[1–3]. Coronavirus (CoV) is a positive-stranded RNA virus and involves the largest viral RNA genome known to date. Phylogenetic studies have shown that SARS-CoV is a previously unknown coronavirus, which is neither a member nor a mutant of any known coronavirus group, and is believed to be a novel human

Abstract

Aim: To characterize enzymatic activity of severe acute respiratory syndrome (SARS) coronavirus (CoV) 3C-like protease (3CL^{pro}) and its four site-directed mutants. **Methods:** Based on the fluorescence resonance energy transfer (FRET) principle using 5-[(2'-aminoethyl)-amino] naphthalenesulfonic acid (EDANS) and 4-[[4-(dimethylamino) phenyl] azo] benzoic acid (Dabcyl) as the energy transfer pair, one fluorogenic substrate was designed for the evaluation of SARS-CoV 3CL^{pro} proteolytic activity. **Results:** The kinetic parameters of the fluorogenic substrate have been determined as $K_m=404 \mu\text{mol}\cdot\text{L}^{-1}$, $k_{\text{cat}}=1.08 \text{ min}^{-1}$, and $k_{\text{cat}}/K_m=2.7 \text{ mmol}^{-1}\cdot\text{L}\cdot\text{min}^{-1}$. SARS-CoV 3CL^{pro} showed substantial pH and temperature-triggered activity switches, and site-directed mutagenesis analysis of SARS-CoV 3CL^{pro} revealed that substitutions of His⁴¹, Cys¹⁴⁵, and His¹⁶³ resulted in complete loss of enzymatic activity, while replacement of Met¹⁶² with Ala caused strongly increased activity. **Conclusion:** This present work has provided valuable information for understanding the catalytic mechanism of SARS-CoV 3CL^{pro}. This FRET-based assay might supply an ideal approach for the exploration SARS-CoV 3CL^{pro} putative inhibitors.

coronavirus, possibly originating from a non-human host^[4].

Proteolytic processing of viral polyproteins is a vital step in the replication cycle of many positive-strand RNA viruses and such processing is commonly performed by virus-genome encoded protease^[5,6]. The open reading frame (ORF) of the coronavirus replicase gene for encoding the proteins which is required for virus replication and transcription, encompasses more than 20 000 nucleotides^[7,8] and encodes two overlapping polyproteins, pp1a (replicase1a, around 450 kDa) and pp1ab (replicase1ab, approximately 750 kDa). It is known that the replicase gene features the sequence motifs of both papain-like protease and 3-chymotrypsin like pro-

tease (3CL^{pro})^[9,10]. 3CL^{pro}, which is also called main protease, functions as a key protease to control the activities of coronavirus replication complexes.

It has been concluded from previous research data that 3CL^{pro}-mediated processing pathways are conserved in coronaviruses. Coronavirus main proteases employ cysteine and histidine residues as the catalytic dyad in the catalytic site but lack a corresponding third catalytic site^[5,11–13], which is an acidic residue in chymotrypsin. Previous research has also confirmed that substrate specificities for the coronavirus main proteases are well defined, with the known proteolytic sites involving bulky hydrophobic residues (mainly leucine/isoleucine) at the P2 position, conserved glutamine at the P1 position, and small aliphatic residues at the P1' position^[14,15]. In addition, secondary structural studies for substrates of SARS-CoV 3CL^{pro} have revealed that substrates with more beta-sheet like structures tend to be cleaved quickly^[16]. The determination of the crystal structures for human coronavirus (strain 229E) 3CL^{pro} and the inhibitor complex of porcine coronavirus (transmissible gastroenteritis virus, TGEV) 3CL^{pro} also confirmed a remarkable degree of conservation of the substrate binding sites for coronavirus 3CL^{pro}^[17]. The recently reported crystal structures of SARS-CoV 3CL^{pro} and its complex with an inhibitor revealed substantial pH-dependant conformational changes that correlate well with the varying activity of 3CL^{pro} at different pH levels, and an unexpected model of inhibitor binding^[18]. In fact, it has already been shown that 3CL^{pro} is an ideal target for screening anti-virus agents^[15,19,20]. Like other 3CL^{pro}, SARS-CoV 3CL^{pro} might become an attractive target in discovering new agents for the treatment of SARS^[17].

In our previous work, we reported a 3D model of SARS-CoV 3CL^{pro} with its inhibitors, designed by virtual screening^[21], and the molecular cloning, expression and purification of SARS-CoV 3CL^{pro}, with a preliminary study on its mass spectral characterization^[22].

To date, the proteolytic activity of SARS-CoV 3CL^{pro} has been almost determined by substrate-analog peptide cleavage assays using conventional RP-HPLC techniques^[16]. In fact, the fluorescence-based assay is another method for quantitative protease activity assay, eg fluorescence resonance energy transfer (FRET) has been successfully used to develop spectrophotometric assays for many proteases^[23–25]. The FRET-based method is more sensitive and less time-consuming compared with the RP-HPLC technique. Recently, a fluorogenic 14-amino acid peptide has been reported to measure SARS-CoV 3CL^{pro} enzymatic activity^[26]. In the present report, we describe how this methodology can be used to design a 12-amino acid fluorogenic peptide with

EDANS/ Dabcyl as the fluorescence quenching pair. This fluorogenic substrate has been successfully used to characterize the proteolytic activities of wild type SARS-CoV 3CL^{pro} at different pH levels and temperatures, and its four site-directed mutants including two catalytic residues and two substrate-binding sites as well. To our knowledge, such a fluorescence-based assay is the first to be used for site-directed mutation analysis of SARS-CoV 3CL^{pro}. We hope that this present FRET-based assay will supply an ideal platform for the exploration of SARS-CoV 3CL^{pro} putative inhibitors.

Materials and methods

Materials All chemicals were of HPLC grade and purchased from Sigma (St Louis, MO). The Ni-NTA chelating affinity column, protease for tag-cleavage and low molecular weight marker for SDS-PAGE were from Amersham Pharmacia Biotech (Uppsala, Sweden).

Cloning, expression and purification of SARS-CoV 3CL^{pro} SARS-CoV 3CL^{pro} was cloned, expressed, and purified, as described by Sun *et al*^[22]. The purified His-tagged SARS-CoV 3CL^{pro} was analyzed by SDS-PAGE, concentrated by centrprep (Milipore), and stored in sodium phosphate 20 mmol·L⁻¹ pH 7.5/NaCl 100 mmol·L⁻¹/dithiothreitol (DTT) 5 mmol·L⁻¹/ethylene diaminetetraacetic acid (EDTA) 1 mmol·L⁻¹ at 4 °C. The structural integrity was analyzed by circular dichroism (CD).

Site-directed mutagenesis of SARS-CoV 3CL^{pro} Site-directed mutagenesis was effected by using a modified recombinant PCR method. Four mutant SARS-CoV 3CL^{pro} (SARS-CoV 3CL^{pro} His⁴¹Ala, Cys¹⁴⁵Ala, His¹⁶³Ala, and Met¹⁶²Ala) were prepared with the QuickChange site-directed mutagenesis kit (Stratagene) using pQE30-SARS-CoV 3CL^{pro} as a template. The nucleotide sequences of the primers used for site-directed mutagenesis were given in Table 1. The pQE30-SARS-CoV 3CL^{pro} plasmids encoding mutant forms of SARS-CoV 3CL^{pro} were verified by sequencing and then transformed into *E coli* M15 cells, and the mutant proteins were expressed and purified in a similar procedure to that for the wild type protease. The purity and structural integrity of the mutant proteins were analyzed by SDS-PAGE. The circular dichroism (CD) spectra of four site-directed mutants were compared with those of wild type SARS-CoV 3CL^{pro} to exclude the possibility of structural misfolding caused by site-directed mutation (data not shown).

Synthesis of fluorogenic substrate The 12-amino acid fluorogenic substrate EDANS-Val-Asn-Ser-Thr-Leu-Gln-Ser-Gly-Leu-Arg-Lys(Dabcyl)-Met was synthesized and

characterized using a modified procedure described by Garcia-Echeverria and Rich^[27]. *N*^α-tert-butyloxycarbonyl (Boc)-protected amino acids were used in all coupling steps. The base liable-protecting group, 9-fluorenylmethoxycarbonyl (Fmoc), was used for the protection of the side chain of lysine, while the benzyl (Bzl) group was employed for the protection of C-terminal carboxyl group of the peptide. The Boc protecting group was removed before coupling by using HCl 4 mol/L in dioxane. Peptide couplings were achieved by overnight reaction with 1,3-dicyclohexylcarbodiimide (DCC) or 1-(3-dimethylaminopropyl)-3-ethylcarbodiimide hydrochloride and 1-hydroxybenzotriazole (HOBT) in *N,N*-dimethylformamide (DMF). After completion of synthesis, the benzyl group was removed by hydrogenolysis in methanol. The commercially available 5-[(2'-aminoethyl)-amino] naphthalenesulfonic acid (EDANS) and 4-[[4-(dimethylamino) phenyl] azo] benzoic acid (Dabcyl) groups were attached to the peptides with conventional condensation reactions^[28], and the Fmoc group was removed from the lysine ε-amine group by treatment with piperidine-*N,N*-dimethylformamide (1:1 v/v) to give the final fluorogenic substrate. The crude products were purified by means of HPLC on a Kromasil 7-μm C₈ column (25 mm×250 mm). The purity of the final products was evaluated by reversed-phase HPLC on a Kromasil 5-μm C₈ column (4.6 mm×250 mm). The integrity of the purified peptides was determined by LCQ-DECA mass spectrometry (ThermoFinnigan, San Jose, CA), and the observed molecular mass was found to agree with the calculated value.

Enzymatic activity assay Stock solution for the fluorogenic substrate was prepared in Me₂SO and stored at 4 °C. Subsequent dilutions were performed using the assay buffer (sodium phosphate 20 mmol/L, pH 7.5, NaCl 100 mmol/L,

DTT 5 mmol/L, EDTA 1 mmol/L) with the final concentration of Me₂SO less than 1 % (v/v).

Initial fluorimetric assays were performed in a 1 mL quartz cuvette with a 1 cm path length at 25 °C. During the assay, SARS-CoV 3CL^{pro} (final concentration 1 μmol/L) was preincubated at 25 °C for 30 min in the cuvette containing the assay buffer, followed by the addition of the fluorogenic substrate stock solutions to a final concentration of 10 μmol/L. The increase in emission fluorescence intensity was recorded at 10 min intervals on a Hitachi F-2500 fluorescence spectrophotometer connected to a thermostat. When fluorescence was being measured, the instrument was first set to zero with the fluorogenic substrate itself in the assay buffer. Cleavage of the peptide as a function of time was followed by monitoring the emission fluorescence intensity at a wavelength of 490 nm upon excitation at 340 nm (slit width 10 nm), and the initial reaction velocity (*v*₀) was determined from the linear portion of the progress curve. The final emission fluorescence intensity of the totally hydrolyzed substrate was determined by adding excess SARS-CoV 3CL^{pro} until no emission fluorescence intensity change at a wavelength of 490 nm was recorded.

Kinetic parameters (*K*_m and *k*_{cat}) of SARS-CoV 3CL^{pro} for the fluorogenic substrate were determined by incubation of the substrate at different concentrations ranging from 1 mmol/L to 5 μmol/L with SARS-CoV 3CL^{pro} 1 μmol/L at 25 °C in the assay buffer. The reaction velocity (*v*₀) for each substrate concentration was averaged from three assay results. *K*_m and *k*_{cat} values were calculated by using a Lineweaver-Burk plot.

The relative enzymatic activity at varying pH levels was investigated at 25 °C in citric acid/phosphate buffer (pH =5, 6, 7, and 8) and glycine/NaOH buffer (pH=9, 10) containing

Table 1. Nucleotide sequences of the primers used for site-directed mutagenesis of SARS-CoV 3CL^{pro}*

Oligonucleotide sequence (5'→3')	Polarity	Mutation introduced
CAGTATACTGTCCAAGAG GCT GTTCATTGACAGCAG	Forward	SARS-CoV 3CL ^{pro} His ⁴¹ Ala
CTGCTGTGCAAAATGAC AG CTCTTGGACAGTATACTG	Reverse	SARS-CoV 3CL ^{pro} His ⁴¹ Ala
GGTCTTTCTTAATGGATCAG CT GGTAGTGTGGTTTTAAC	Forward	SARS-CoV 3CL ^{pro} Cys ¹⁴⁵ Ala
GTAAACCAACACTACC AG CTGATCCATTAAGGAAAGAACC	Reverse	SARS-CoV 3CL ^{pro} Cys ¹⁴⁵ Ala
GTGTCTTTCTGCTATATGG CT CATATGGAGCTTCCAACAGG	Forward	SARS-CoV 3CL ^{pro} His ¹⁶³ Ala
CCTGTTGGAAGCTCCATATG AG CCATATAGCAGAAAGACAC	Reverse	SARS-CoV 3CL ^{pro} His ¹⁶³ Ala
GCGTGTCTTTCTGCTAT GCG CATCATATGGAGCTTCC	Forward	SARS-CoV 3CL ^{pro} Met ¹⁶² Ala
GGAAGCTCCATATGAT GCG CATAGCAGAAAGACACGG	Reverse	SARS-CoV 3CL ^{pro} Met ¹⁶² Ala

* The mutant codons in the oligonucleotide sequences are highlighted in boldface. SARS-CoV 3CL^{pro} amino acids are numbered continuously from the N-terminal residue, Ser¹, to the C-terminal residue, Gln³⁰³.

DTT 5 mmol/L, EDTA 1 mmol/L, SARS-CoV 3CL^{pro} 1 μmol/L and fluorogenic substrate 10 μmol/L. The reaction velocity (v_0) at each pH value was measured in triplicate and averaged.

The enzymatic activity at different temperatures (10, 20, 30, 40, and 50 °C) was measured in an assay buffer containing SARS-CoV 3CL^{pro} 1 μmol·L⁻¹ and substrate 10 μmol/L. The enzyme was equilibrated at the same temperature as that for the assay buffer and substrate solution before mixing. During the assay, the cuvette temperature was stabilized by a thermostat connected to a Hitachi F-2500 fluorescence spectrophotometer. The reaction velocity (v_0) at each temperature was the average of the three parallel assays and the reaction velocity at 40 °C was taken as 1.0.

The enzymatic activity of four site-directed mutants of SARS-CoV 3CL^{pro} (SARS-CoV 3CL^{pro} His⁴¹Ala, Cys¹⁴⁵Ala, His¹⁶³Ala, and Met¹⁶²Ala) was the average of three parallel assays performed in an identical way as described above for wild type SARS-CoV 3CL^{pro}.

Results and discussion

Fluorogenic substrate design and initial fluorimetric assay It is well established that the specificities of CoV 3CL^{pro} for the substrate involves bulky hydrophobic residues (mainly leucine/isoleucine) at the P2 position, conserved glutamine at the P1 position, and small aliphatic residues at the P1' position. A 12-amino acid peptide representing the NH₂-terminal autoprocessing site of TGEV 3CL^{pro} with the sequence of substrate-analog chloromethyl ketone inhibitor Cbz-Val-Asn-Ser-Thr-Leu-Gln-CMK was devised to separate the quencher from the fluorescent donor chromophore for designing the fluorogenic substrate in this study (Figure 1A), considering that a published cleavage experiment found that a 15-amino acid substrate involving these sequences could be efficiently cleaved by SARS-CoV 3CL^{pro}[17]. To ensure efficient internal quenching, a commercially available donor/quencher pair was chosen for this study: 5-[(2'-aminoethyl)-amino] naphthalenesulfonic acid (EDANS) and 4-[[4-(dimethylamino) phenyl] azo] benzoic acid (Dabcyl) (Figure 1B). These dyes had already been used in FRET-based procedures^[25,29,30]. Most importantly, the EDANS/Dabcyl pair possessed adequate spectral overlap which allowed almost complete quenching of EDANS's fluorescence. The detailed experimental procedure for characterizing the enzymatic activity of SARS-CoV 3CL^{pro} was illustrated in Figure 2.

To evaluate the availability of the synthesized peptide as a potential substrate of SARS-CoV 3CL^{pro}, an initial fluo-

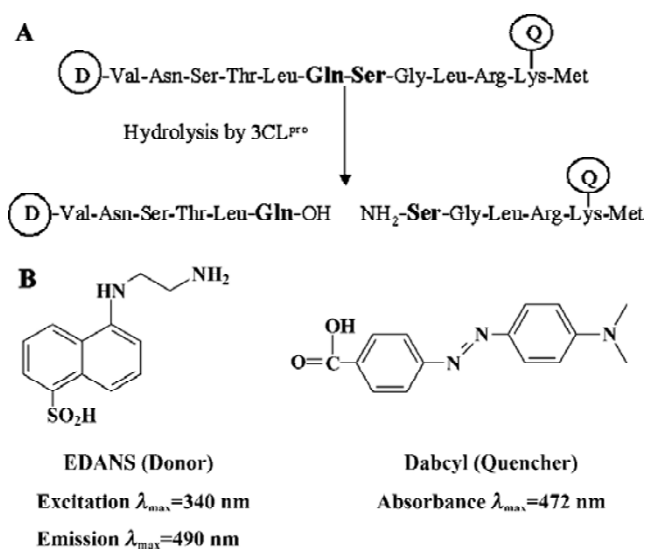


Figure 1. (A) Proposed design of fluorogenic substrate. Cleavage site is highlighted in boldface; D, the fluorescent donor chromophore; Q, quencher. (B) Structures and fluorescent properties of the donor/quencher pair EDANS/Dabcyl.

rimetric assay was performed. Comparison of the fluorescence emission spectrum of only the fluorogenic substrate (data not shown) with those spectra incubated with SARS-CoV 3CL^{pro} (Figure 3A) clearly showed that the Dabcyl group almost exclusively quenched the donor emission of the EDANS fluorophore in the fluorogenic substrate and the fluorogenic substrate was efficiently hydrolyzed by SARS-CoV 3CL^{pro}. The obvious emission fluorescence intensity enhancement over time implies that the fluorogenic substrate is ideal for subsequent enzymatic activity assays against SARS-CoV 3CL^{pro}.

Enzymatic activity assays Considering the data obtained from the initial fluorimetric assay, SARS-CoV 3CL^{pro} proteolysis against the fluorogenic substrate resulted in an appreciable increase in emission fluorescence intensity at a wavelength of 490 nm as a function of time, and a typical fluorescence profile following hydrolysis of the substrate is shown in Figure 3B. As a control, incubation of the substrate in assay buffer in the absence of SARS-CoV 3CL^{pro} showed no fluorescence intensity change over time (data not shown).

Measurement of the kinetic parameters (K_m and k_{cat}) was accomplished by conducting hydrolysis of the fluorogenic substrate at various concentrations. A typical Lineweaver-Burk plot is shown in Figure 4, which plots the reciprocal of the initial velocity (v_0) versus the reciprocal of the substrate concentration. The data for each concentration were ob-

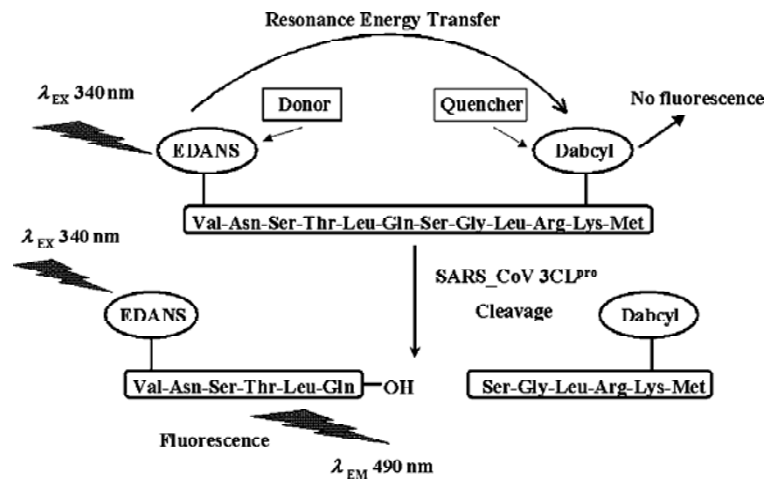


Figure 2. The experimental procedure of enzymatic activity characterization of SARS-CoV 3CL^{pro} using the fluorogenic substrate.

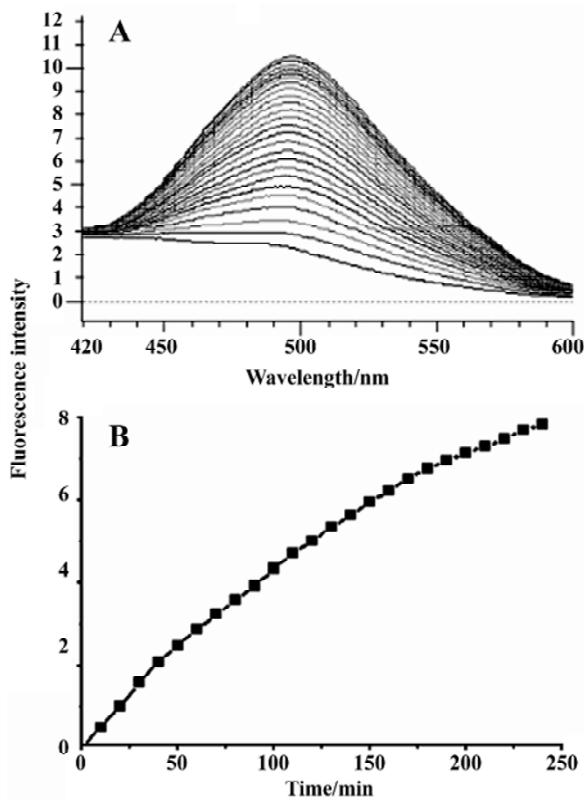


Figure 3. Initial fluorimetric assay and representative fluorescence profile of hydrolysis of the substrate by SARS-CoV 3CL^{pro}. (A) Emission spectra of the synthesized substrate incubated with SARS-CoV 3CL^{pro} recorded at 10 min intervals; $\lambda_{EX} = 340$ nm; $\lambda_{peak EM} = 490$ nm. (B) The initial reaction velocity (v_0) was determined from the linear portion of the progress curve, which corresponded to between 2% and 10% hydrolysis of the substrate.

tained in triplicate. The calculated K_m and k_{cat} values were

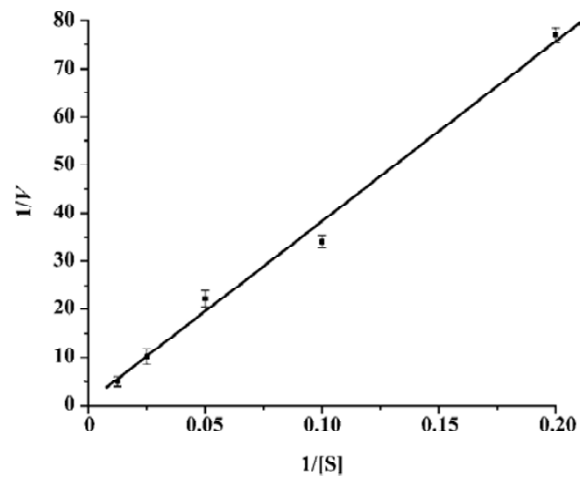


Figure 4. Determination of the kinetic parameters (K_m and k_{cat}) by Lineweaver-Burk plot. Enzymatic activity at different substrate concentrations varying from 1 mmol/L to 5 μ mol/L was measured. The K_m and k_{cat} values were calculated by linear fitting method using ORIGIN 7.0. V: μ mol \cdot L⁻¹ \cdot min⁻¹; S: μ mol \cdot L⁻¹.

404 \pm 9 μ mol/L and 1.08 \pm 0.14 min⁻¹, respectively. Obviously, the relatively small k_{cat}/K_m value (2.7 \pm 0.3 mmol⁻¹ \cdot L \cdot min⁻¹) indicated that the *in vitro* activity of SARS-CoV 3CL^{pro} was low, in common with other reported coronavirus 3CL^{pro}[5]. Such a low activity for SARS-CoV 3CL^{pro} may be due to the fact that only the dimer of 3CL^{pro} was the active form, and efficient active dimeric form was often at relatively low concentrations during the enzyme assay^[16,26].

Figure 5 showed the results concerning the relative enzymatic activity at various pH values for SARS-CoV 3CL^{pro}. The protease exhibited a stable proteolytic activity at pH 7.0–x9.0, and displayed only 50% activity at pH 6.0 and 10.0.

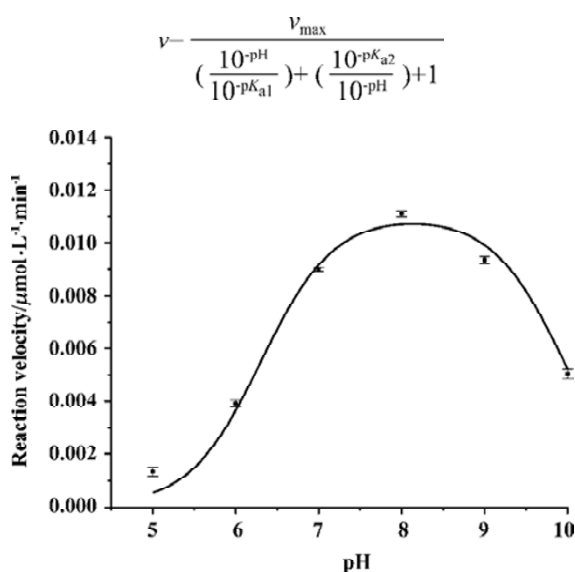


Figure 5. Enzymatic activity of SARS-CoV 3CL^{pro} at different pH. The reaction velocity (v_0) was determined in citric acid/phosphate buffer (pH=5, 6, 7, 8) or glycine/NaOH buffer (pH=9, 10). The curve was fitted by an equation described by Copeland^[32] using ORIGIN 7.0.

However, when pH decreased to 5.0, it almost lost its activity completely. These results were strongly supported by a recent study, which discussed the pH dependence and the catalytic mechanism of SARS-CoV 3CL^{pro}^[31]. The pH profile shown in Figure 5 can be fitted by the following equation^[32]:

Where v is the measured reaction velocity that is plotted on the y axis, v_{\max} is the observed maximum value of the reaction velocity, and pK_{a1} and pK_{a2} refer to the pK_a values for the two relevant acid-base catalytic groups being titrated. A fit of the curve in Fig 5 to the equation yielded values of pK_{a1} and pK_{a2} of 6.31 ± 0.12 and 9.95 ± 0.11 , respectively, and Cys¹⁴⁵ formed a catalytic dyad in the active site of SARS-CoV 3CL^{pro}, and ionization of sulfhydryl group of Cys¹⁴⁵ and imidazole group of His⁴¹ played an important role in catalytic processing of substrate hydrolysis^[18].

The relative enzymatic activity of SARS-CoV 3CL^{pro} at different temperatures was depicted in Figure 6; the activity of SARS-CoV 3CL^{pro} nearly doubled with every 10 °C increase from 10 to 40 °C, and such a result accorded well with the thermodynamics of a typical chemical reaction. Like all proteins, SARS-CoV 3CL^{pro} undergoes thermal denaturation at elevated temperatures, hence the increases in the catalytic efficiency of the protease with increasing temperature might be compromised by the competing effects of the enzyme denaturation at high temperature. As indicated in Figure 6, the enzymatic activity diminished significantly at

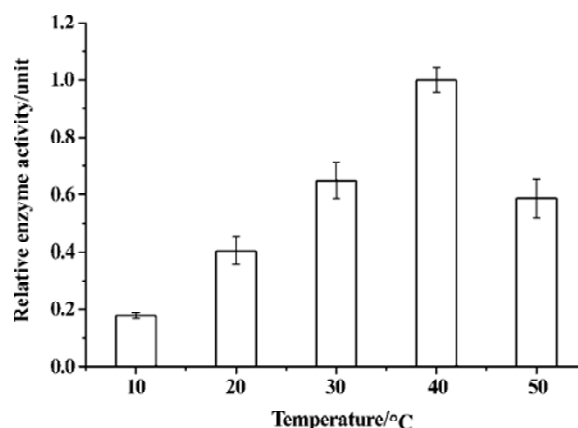


Figure 6. Enzymatic activity of SARS-CoV 3CL^{pro} at varying temperatures. The reaction velocity (v_0) was determined at 10, 20, 30, 40 and 50 °C respectively. The reaction velocity (v_0) at 40 °C was taken as 1.0.

50 °C which was consistent with thermal denaturation of SARS-CoV 3CL^{pro} as monitored by circular dichroism^[16].

Mutation analysis of the catalytic dyad and two substrate-binding residues Based on the sequence alignments, previous mutagenesis studies with other CoV 3CL^{pro}^[7,9,33,34] and the recently reported crystal structure of SARS-CoV 3CL^{pro}^[18], the two residues His⁴¹ and Cys¹⁴⁵ are fully conserved and considered to be the principal catalytic residues of CoV 3CL^{pro}. Therefore, to confirm these two residues' functions in the enzymatic activity of SARS-CoV 3CL^{pro}, both residues were mutated into Ala. As indicated in Table 2, the proteolytic activity in SARS-CoV 3CL^{pro} His⁴¹Ala and Cys¹⁴⁵Ala mutants were below the detection limit of the enzyme assay, which suggested a complete loss of enzymatic activities for these two mutants. Furthermore, these data strongly supported an indispensable catalytic function for His⁴¹ and Cys¹⁴⁵, and were fully consistent with the mutagenesis data analysis published previously on the HCoV, IBV, MHV, and FIPV 3CL^{pro}^[5,11,35,36].

Additionally, it has been proposed that coronavirus 3CL^{pro} might employ the characteristic sequence signature Tyr¹⁶¹-Met¹⁶²-His¹⁶³ for substrate binding^[33]. However, to date, this theoretical functional character has not been tested experimentally for SARS-CoV 3CL^{pro}. The need for experimental data becomes more evident considering the relatively low sequence identity between SARS-CoV 3CL^{pro} and 3CL^{pro} of other coronavirus groups. With these facts in mind, we focused on the Met¹⁶² and His¹⁶³ residues of SARS-CoV 3CL^{pro} by site-directed mutagenesis analysis.

First of all, we exchanged Ala for the conserved His¹⁶³.

Table 2. Enzymatic activities of wild type and site-directed mutants of SARS-CoV 3CL^{pro}*

Protein	Proteolytic activity/%
SARS-CoV 3CL ^{pro}	100 %
SARS-CoV 3CL ^{pro} His ⁴¹ Ala	<1 %
SARS-CoV 3CL ^{pro} Cys ¹⁴⁵ Ala	<1 %
SARS-CoV 3CL ^{pro} His ¹⁶³ Ala	<1 %
SARS-CoV 3CL ^{pro} Met ¹⁶² Ala	182 %

* Enzymatic activities were averages determined in three parallel experiments. The activity of wild type SARS-CoV 3CL^{pro} was taken as 100 %.

As shown in Table 2, the proteolytic activity of this mutant dropped below the detection limit of the enzyme assay. Such an obvious indispensability of His¹⁶³ for proteolytic activity supported the conclusion that His¹⁶³ remained uncharged at physiological pH to facilitate optimal interaction with the Gln-P1 of the substrate in substrate-binding subsite S1 as determined by the recently reported crystal structure of SARS-CoV 3CL^{pro} [18]. This was also consistent with the mutagenesis data obtained previously for the same His residue in other CoV 3CL^{pro}[36]. Secondly, when Met¹⁶² residue was substituted with Ala, it was found that such a mutation did not decrease the proteolytic activity. On the contrary, it exhibited strongly increased activity: almost double compared with the wild type SARS-CoV 3CL^{pro}. This result was consistent with the corresponding research for FIBV 3CL^{pro} [36], and indicated that Met¹⁶² was not indispensable for proteolytic activity even though it was conserved among CoV 3CL^{pro}. It was tentatively suggested that such an increase of proteolytic activity for SARS-CoV 3CL^{pro} caused by Met¹⁶² mutation might be due to the fact that the substitution changed the spatial properties of the substrate-binding subsite S1 and facilitated substrate binding.

In summary, in this report, based on FRET theory, a fluorogenic substrate for detection of proteolytic activity of SARS-CoV 3CL^{pro} was successfully synthesized and evaluated. The kinetic parameters showed that the *in vitro* activity of SARS 3CL^{pro} was relatively low, perhaps due to the low concentration of the active dimeric form under the enzyme assay conditions. The pH profile of enzymatic activity yielded pK_{a1} and pK_{a2} values of 6.2 and 10.0, respectively, which correlated well with the finding that ionization of the catalytic dyad of His⁴¹ and Cys¹⁴⁵ was perhaps vital during the catalytic processing of substrate hydrolysis. In addition, SARS-CoV 3CL^{pro} displayed nearly a twofold

increase in activity with every 10 °C increase at 10–40 °C, and diminished its activity significantly at 50 °C owing to thermal denaturation. Mutation analysis revealed that substitution of either His⁴¹ and Cys¹⁴⁵ residues resulted in complete loss of proteolytic activity, which was also observed for the residue His¹⁶³ in the substrate-binding subsite S1. Replacement of Met¹⁶² with Ala caused increased activity, although the detailed mechanism was still unknown. The present FRET-based assay might supply an ideal platform for the exploration of SARS-CoV and other CoV 3CL^{pro} putative inhibitors, given the conserved substrate specificities of CoV 3CL^{pro}.

References

- Holmes KV. SARS coronavirus: a new challenge for prevention and therapy. *J Clin Invest* 2003; 111: 1605–9.
- Peiris JS, Lai ST, Poon LL, Guan Y, Yam LY, Lim W, *et al*. Coronavirus as a possible cause of severe acute respiratory syndrome. *Lancet* 2003; 361: 1319–25.
- Fouchier RA, Kuiken T, Schutten M, Van Amerongen G, Van Doornum GJ, Van Den Hoogen BG, *et al*. Aetiology: Koch's postulates fulfilled for SARS virus. *Nature* 2003; 423: 240–7.
- Holmes KV. SARS-associated coronavirus. *N Engl J Med* 2003; 348: 1948–51.
- Ziebuhr J, Heussipp G, Siddell SG. Biosynthesis, purification, and characterization of the human coronavirus 229E 3C-like proteinase. *J Virol* 1997; 71: 3992–7.
- Dougherty WG, Semler BL. Expression of virus-encoded proteinases: functional and structural similarities with cellular enzymes. *Microbiol Rev* 1993; 57: 781–822.
- Eleouet JF, Rasschaert D, Lambert P, Levy L, Vende P, Laude H. Complete sequence (20 kilobases) of the polyprotein-encoding gene 1 of transmissible gastroenteritis virus. *Virology* 1995; 206: 817–22.
- Thiel V, Herold J, Schelle B, Siddell SG. Viral replicase gene products suffice for coronavirus discontinuous transcription. *J Virol* 2001; 75: 6676–81.
- Herold J, Raabe T, Schelle-Prinz B, Siddell SG. Nucleotide sequence of the human coronavirus 229E RNA polymerase locus. *Virology* 1993; 195: 680–91.
- Lee HJ, Shieh CK, Gorbalenya AE, Koonin EV, Monica N, Tuler J, *et al*. The complete sequence (22 kilobases) of murine coronavirus gene 1 encoding the putative proteases and RNA polymerase. *Virology* 1991; 180: 567–82.
- Liu DX, Brown TD. Characterization and mutational analysis of an ORF 1a-encoding proteinase domain responsible for proteolytic processing of the infectious bronchitis virus 1a/1b polyprotein. *Virology* 1995; 209: 420–7.
- Ziebuhr J, Snijder EJ, Gorbalenya AE. Virus-encoded proteinases and proteolytic processing in Nidovirales. *J Gen Virol* 2000; 81: 853–79.
- Hegyi A, Ziebuhr J. Conservation of substrate specificities among coronavirus main proteases. *J Gen Virol* 2002; 83: 595–9.
- Ziebuhr J, Herold J, Siddell SG. Characterization of a human coronavirus (strain 229E) 3C-like proteinase activity. *J Virol* 1995;

- 69: 4331–8.
- 15 Anand K, Plam GJ, Mesters JR, Siddell SG, Ziebuhr J, Hilgenfeld R. Structure of coronavirus main proteinase reveals combination of a chymotrypsin fold with an extra alpha-helical domain. *EMBO J* 2002; 21: 3213–24.
 - 16 Fan KQ, Wei P, Feng Q, Chen SD, Huang CK, Ma L, *et al*. Biosynthesis, purification, and substrate specificity of severe acute respiratory syndrome coronavirus 3C-like proteinase. *J Biol Chem* 2004; 279: 1637–42.
 - 17 Anand K, Ziebuhr J, Wadhvani P, Mesters JR, Hilgenfeld R. Coronavirus main proteinase (3CL^{pro}) structure: basis for design of anti-SARS drugs. *Science* 2003; 300: 1763–7.
 - 18 Yang HT, Yang MJ, Ding Y, Liu YW, Lou ZY, Zhou Z, *et al*. The crystal structures of severe acute respiratory syndrome virus main protease and its complex with an inhibitor. *Proc Natl Acad Sci USA* 2003; 100: 13190–5.
 - 19 Kim JC, Spence RA, Currier PF, Liu X, Denison MR. Coronavirus protein processing and RNA synthesis is inhibited by the cysteine protease inhibitor E43d. *Virology* 1995; 208: 1–8.
 - 20 Someya Y, Takeda N, Miyamura T. Identification of active-site amino acid residues in the Chiba virus 3C-like protease. *J Virol* 2002; 76: 5949–58.
 - 21 Xiong B, Gui CS, Xu XY, Luo C, Chen J, Luo HB, *et al*. A 3D model of SARS-CoV 3CL proteinase and its inhibitors design by virtual screening. *Acta Pharmacol Sin* 2003; 24: 497–504.
 - 22 Sun HF, Luo HB, Yu CY, Sun T, Chen J, Peng SY, *et al*. Molecular cloning, expression, purification, and mass spectrometric characterization of 3C-like protease of SARS coronavirus. *Protein Exp Purif* 2003; 32: 302–8.
 - 23 Knight CG, Willenbrock F, Murphy G. A novel coumarin-labelled peptide for sensitive continuous assays of the matrix metalloproteinases. *FEBS Lett* 1992; 296: 263–6.
 - 24 Angliker H, Neumann U, Molloy SS, Thomas G. Internally quenched fluorogenic substrate for furin. *Anal Biochem* 1995; 224: 409–12.
 - 25 Mittoo S, Sundstrom LE, Bradley M. Synthesis and evaluation of fluorescent probes for the detection of calpain activity. *Anal Biochem* 2003; 319: 234–8.
 - 26 Kuo CJ, Chi YH, Hsu JT, Liang PH. Characterization of SARS main protease and inhibitor assay using a fluorogenic substrate. *Biochem Biophys Res Commun* 2004; 318: 862–7.
 - 27 Garcia-Echeverria C, Rich DH. New intramolecularly quenched fluorogenic peptide substrates for the study of the kinetic specificity of papain. *FEBS Lett* 1992; 297: 100–2.
 - 28 Wang GT, Matayoshi E, Jan Huffaker H, Krafft GA. Design and synthesis of new fluorogenic HIV protease substrates based on resonance energy transfer. *Tetrahedron Lett* 1990; 31: 6493–6.
 - 29 Matayoshi ED, Wang GT, Krafft GA, Erickson J. Novel fluorogenic substrates for assaying retroviral proteases by resonance energy transfer. *Science* 1990; 247: 954–8.
 - 30 Maggiora LL, Smith CW, Zhang ZY. A general method for the preparation of internally quenched fluorogenic protease substrates using solid-phase peptide synthesis. *J Med Chem* 1992; 35: 3727–30.
 - 31 Huang CK, Wei P, Fan KQ, Liu Y, Lai LL. 3C-like proteinase from SARS coronavirus catalyzes substrate hydrolysis by a general base mechanism. *Biochemistry* 2004; 43: 4568–74.
 - 32 Copeland RA. *Enzymes: A Practical Introduction to Structure, Mechanism, and Data Analysis*. 2nd ed. New York: Wiley-VCH Inc; 2000.
 - 33 Gorbalenya AE, Koonin EV, Donchenko AP, Blinov VM. Coronavirus genome: prediction of putative functional domains in the non-structural polyprotein by comparative amino acid sequence analysis. *Nucleic Acids Res* 1989; 17: 4847–61.
 - 34 Marra MA, Jones SJM, Astell CR, Holt RA, Wilson AB, Butterfield YSN, *et al*. The genome sequence of the SARS-associated coronavirus. *Science* 2003; 300: 1399–403.
 - 35 Lu Y, Denison MR. Determinants of mouse hepatitis virus 3C-like proteinase activity. *Virology* 1997; 230: 335–42.
 - 36 Hegyi A, Friebe A, Gorbalenya AE, Ziebuhr J. Mutational analysis of the active centre of coronavirus 3C-like proteases. *J Gen Virol* 2002; 83: 581–93.